ACCSCIENCE PUBLISHING

International Journal of Bioprinting

RESEARCH ARTICLE

# Patient-specific design and fabrication of a trapeziometacarpal joint orthosis using a computed tomography image-based finite element model

**Chan Beom Park[1†], Ji Sup Hwang[2†], Hyun Sik Gong[3*], and Hyung-Soon Park[1*]**

[1]Department of Mechanical Engineering, Korea Advanced Institute of Science and Technology, Daejeon, South Korea

[2]Department of Orthopedic Surgery, Seoul National University Hospital, Seoul, South Korea

[3]Department of Orthopedic Surgery, Seoul National University College of Medicine, Seoul National University Bundang Hospital, Seongnam-si, South Korea

## Abstract

Osteoarthritis (OA) of the trapeziometacarpal joint (TMCJ) can be caused by biomechanical wear on the articular cartilage due to high joint contact pressure, leading to severe pain in the thumb. Static orthoses have been applied for treatment in the early stages of OA to immobilize the TMCJ in a comfortable posture, but they do not account for contact pressure at the TMCJ. This oversight results in a high failure rate in pain relief during splinting. To ensure successful treatment, it is desirable to immobilize the TMCJ in an optimal posture that minimizes biomechanical joint contact pressure. This paper presents a patient-specific TMCJ orthosis design for the optimal posture, based on joint contact pressure obtained from a computed tomography image-based finite element (FE) TMCJ model. The estimated pressure at the subject-specific optimal posture averaged 2.8E-3 MPa, which was lower compared to the average pressure of 3.2E-2 MPa at the non-optimal but comfortable posture. To maintain this subject-specific optimal TMCJ posture, the orthosis was designed based on individual hand geometries with three-dimensional (3D) printing technology. The 3D-printed orthosis was preliminarily evaluated by patients with moderate to severe OA, and all patients reported pain relief. The visual analog scale and disabilities of arm, shoulder, and hand scores improved by 1.8 ± 1.7 and 13.1 ± 5.4, respectively. For orthotic treatment in clinics, the FE model-based TMCJ orthosis design for the subject-specific optimal posture can relieve pain caused by OA.

***Keywords:*** 3D printing; Computed tomography; Finite element model; Orthosis; Osteoarthritis; Patient-specific; Trapeziometacarpal joint

†These authors contributed equally to this work

***Corresponding authors:**
Hyun Sik Gong
(hsgong@snu.ac.kr)

Hyung-Soon Park
(hyungspark@kaist.ac.kr)

**Citation:** Park CB, Hwang JS, Gong HS, Park HS. Patient-specific design and fabrication of a trapeziometacarpal joint orthosis using a computed tomography image-based finite element model. *Int J Bioprint*. 2025;11(1):233-245. doi: 10.36922/ijb.4635

Received: August 23, 2024
Revised: September 22, 2024
Accepted: October 7, 2024
Published Online: October 8, 2024

**Copyright:** © 2024 Author(s). This is an Open Access article distributed under the terms of the Creative Commons Attribution License, permitting distribution, and reproduction in any medium, provided the original work is properly cited.

**Publisher's Note:** AccScience Publishing remains neutral with regard to jurisdictional claims in published maps and institutional affiliations.

## 1. Introduction

Osteoarthritis (OA) of the trapeziometacarpal joint (TMCJ), the most proximal joint comprising the thumb, is found in 33% of the population older than 50 years of age.[1] The pathogenesis of TMCJ OA is still not completely understood. One significant cause

is laxity in the TMCJ ligaments, which induces structural instability and results in abnormally increased joint contact pressure on the articular cartilage of the TMCJ during movements.[1] This high joint contact pressure causes cartilage degeneration by biomechanical wear, leading to OA with pain.[2–4]

In the early stages of OA, a static orthosis can be applied for pain relief. Considering that high joint contact pressure, which can be estimated using reconstructed finite element (FE) joint models,[5–8] is a primary biomechanical factor causing OA,[2–4] it is desirable to design the orthosis to immobilize the TMCJ in an optimal posture that minimizes joint contact pressure. This optimal TMCJ posture would vary for each individual due to differences in TMCJ geometries. Immobilizing the TMCJ in the individual optimal posture determined using an FE joint model may prevent further biomechanical cartilage wear due to the minimized contact pressure, thus alleviating pain at rest during splinting. For OA treatment, various static orthoses[9–18] have been developed.

Conventional orthoses have limited capability in achieving pain relief, as they typically immobilize the TMCJ in postures determined solely based on subjective comfort reported by patients. Despite reports indicating positive effects on pain relief and functional improvement during splinting,[9–11,13–15,17,18] orthoses designed based on subjective comfort during a brief hospital visit can lead to failure in pain relief at rest during splinting.[19–21] Non-optimal TMCJ postures with high joint contact pressure can be misperceived as comfortable and used for splinting because subjective comfort, significantly correlated with pain,[22] is influenced by emotional factors.[22,23] Therefore, a patient-specific orthosis design based on joint contact pressure using an FE model of the TMCJ is required to ensure that the TMCJ is maintained in the subject-specific optimal posture for minimal pressure. In this orthosis design process, three-dimensional (3D) printing technology[15,16,24–28] facilitates the fabrication of orthoses with varying geometries.

The main objective of this paper is to present a novel 3D printing design process for a patient-specific TMCJ orthosis by using an individual FE model-based joint contact pressure analysis to maintain the TMCJ in the subject-specific optimal posture that minimizes the pressure for successful pain relief, which was verified through pain assessment in a clinical setup. The FE method (FEM) was utilized to determine the individual optimal posture with an FE TMCJ model constructed from computed tomography (CT) images, and the orthosis was fabricated based on individual TMCJ geometries with the aid of 3D printing to maintain the optimal TMCJ posture during splinting. The capability of the proposed orthosis in relieving pain at rest was preliminarily evaluated in patients with TMCJ OA. The study includes an overview of the orthosis design process and evaluation method, followed by an assessment of its significance.

## 2. Materials and methods

### 2.1. Overall design process

The orthosis is primarily designed to ensure successful pain relief at rest during splinting by allowing patients to maintain the optimal TMCJ posture (Figure 1). The design steps for making the orthosis comprise (i) FE modeling of the individual TMCJ model, (ii) FE simulation for the optimal posture, and (iii) fabrication of the orthosis via 3D printing.

The individual FE TMCJ model is constructed using CT images of the thumb affected by OA. The constructed FE TMCJ model comprises the metacarpal, the trapezium, attached cartilages, and two fixed rotation axes[29,30] of the metacarpal. The cartilage of the metacarpal is set to move around the fixed cartilage of the trapezium via two rotation axes—flexion-extension (F/E) and abduction-adduction (A/A)—determined based on a reported geometric relationship with the trapezium[31] (details denoted in **Section 2.2**). Since opposition postures were considered undesirable due to the resulting high joint contact pressure,[32] pronation-supination movements required for opposition were excluded from the model. The cartilage movement results in varying contact pressure between the two cartilages.

The optimal TMCJ posture is determined by analyzing joint contact pressure on the cartilages using the constructed individual FE TMCJ model and FEM. As the cartilages glide, the TMCJ posture changes and the joint contact pressure is analyzed at various TMCJ postures using the FEM. Subsequently, the optimal TMCJ posture, which minimizes joint contact pressure, is determined among these postures for each individual.

A static TMCJ orthosis is custom-fabricated for each individual to immobilize the TMCJ in the optimal posture. Prior to modeling the orthosis, a 3D hand model posed in the optimal posture is constructed from CT images. The orthosis is then modeled to cover the 3D hand model, and the modeled orthosis is rigidly 3D-printed. This design ensures that individuals can maintain the optimal posture during splinting.

### 2.2. FE modeling of the individual TMCJ

An individual thumb affected by OA was scanned using a Brilliance iCT 256 CT scanner (Philips Medical Systems, the Netherlands) to construct the FE TMCJ model. Three different postures were scanned (Figure 2A): "neutral,"

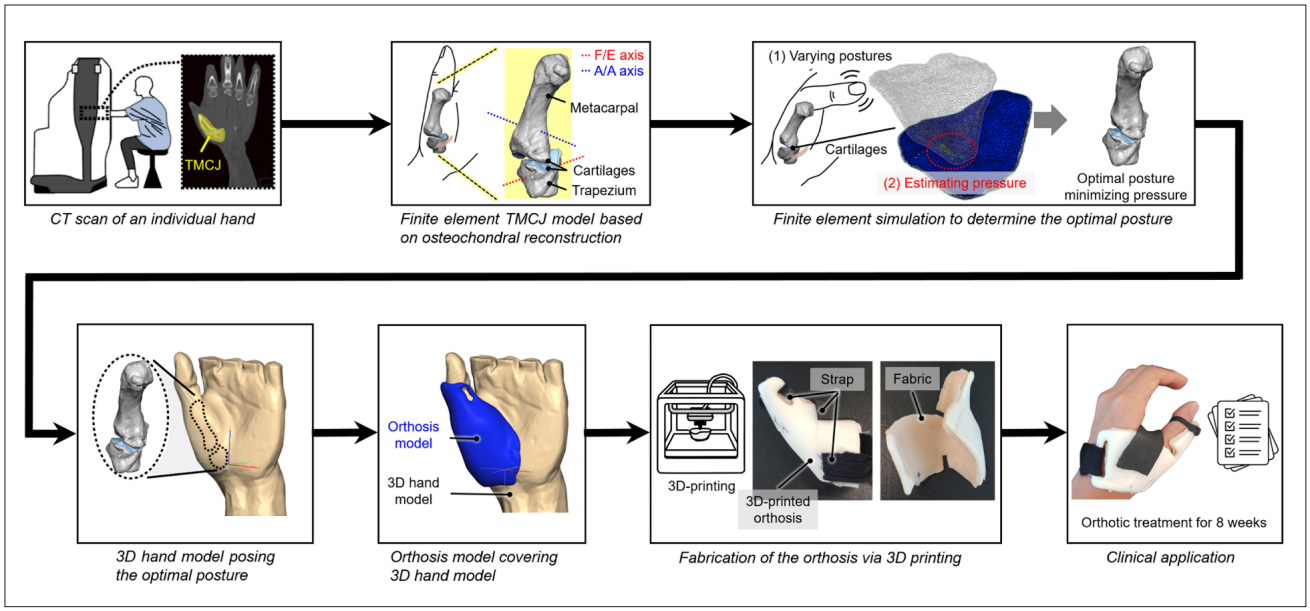


**Figure 1.** The design process used for the patient-specific TMCJ orthosis. The optimal posture that minimizes biomechanical joint contact pressure is determined for each individual using the FEM and an FE TMCJ model constructed from CT images. Subsequently, the orthosis is fabricated via 3D printing to enable patients to maintain the optimal posture during splinting. Abbreviations: A/A, abduction-adduction; CT, Computed tomography; F/E, Flexion-extension; FE, finite element; FEM, finite element method; TMCJ, trapeziometacarpal joint.

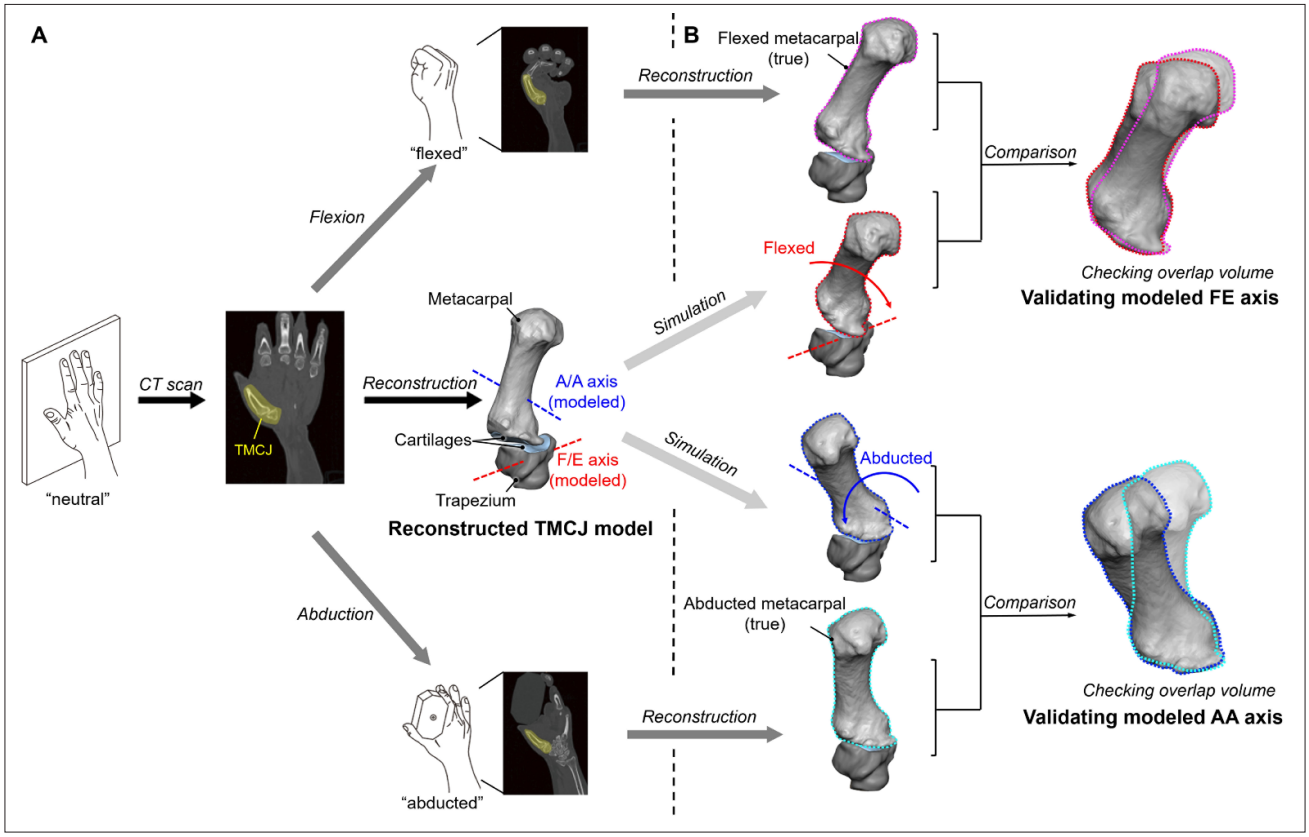


**Figure 2.** Construction of an individual FE TMCJ model. (A) The individual FE TMCJ model is constructed from CT images captured when the TMCJ is in the "neutral" posture. (B) The locations of determined rotation axes of the metacarpal are validated using the metacarpal reconstructed from CT images captured when the TMCJ is in the "flexed" and "abducted" postures. Abbreviations: A/A, abduction-adduction; CT, Computed tomography; F/E, Flexion-extension; FE, finite element; FEM, finite element method; TMCJ, trapeziometacarpal joint.

maintained in a fully extended posture by a flat object; "flexed," maintained in a thumb-in-fist position; and "abducted," maintained by holding a thick object. The following scanning protocol was used for the measurement: 120 kVp tube potential; 149 mAs tube current–time product; 128 × 0.625 mm section collimation; 0.5 ms rotation time; 0.4 pitch; 180 mm display field of view; pixel size of 0.3 × 0.3 mm; and 1-mm section thickness.

The individual FE TMCJ model was constructed using CT images. The metacarpal and the trapezium, along with their attached cartilages, were reconstructed from the CT images of the "neutral" posture using Mimics software (Materialise, Ltd, Belgium), obtaining articulating surface geometries of the cartilages. Due to the challenge in measuring the spatial thickness of thin cartilages using CT images,[33] the cartilages were reconstructed based on the surface geometries and the previously reported cartilage thickness from an *in vivo* study[2] using Geomagic Freeform software (3D Systems, Inc., United States of America [USA]). Note that these thickness values would not significantly affect FEM-based joint contact pressure analysis results, as joint contact pressure is estimated based on the indented distance from the measured articulating surfaces and their contact stiffness. The reconstructed metacarpal, trapezium, and cartilages were then imported into ABAQUS (version 6.14; Dassault Systèmes Simulia Corp., USA) software for FE analysis.

Locations of the rotation axes of the metacarpal were determined and fixed based on their geometric relationships with the trapezium.[29–31] To set the rotation axes, an origin of a global Cartesian coordinate was placed at the base of the trapezium with adjustment of its axes (+*x*, +*y*, and +*z*) respectively towards the palmar, radial, and distal directions.[31] The global Cartesian coordinate was then translated and rotated according to the reported Denavit–Hartenberg parameters,[31] and moved *z*-axes of the coordinates were respectively set as the F/E and A/A rotation axes.

The locations of rotation axes were validated using the reconstructed TMCJ from CT images of the "flexed" and "abducted" postures (Figure 2B). For the validation, it was confirmed whether the rotated metacarpal in the constructed FE TMCJ model overlapped with the metacarpal reconstructed from the CT images of the "flexed" and "abducted" postures. The overlap volume ratio was calculated as the volume of the overlap region divided by the volume of the reconstructed metacarpal from the "neutral" posture (**Equation I**). As it was reported that a structure reconstructed from CT images can have volume variation within ~8% of its volume,[34] it was calculated that a true rotation axis can result in a minimum overlap volume ratio of 85.2% by **Equation I**. Thus, the threshold for the overlap volume ratio was set as 80%, which was closed to the minimum of 85.2%. The global Cartesian coordinate located at the base of the trapezium was adjusted to ensure that the calculated overlap volume ratio exceeded the threshold. The rotation axes satisfying the threshold requirement were then used for the individual FE TMCJ model. Note that the rotation axes of the TMCJ were fixed based on the negligible translation of the metacarpal observed in CT images and reported on its kinematics with OA.[35,36]

$$Overlap\ volume\ ratio\ (\%) = \frac{Volume\ of\ the\ overlap\ region}{Volume\ of\ the\ metacarpal\ from\ "neutral"} \times 100 \quad (I)$$

### 2.3. FE simulation for the optimal posture

To obtain joint contact pressure at various TMCJ postures via FE simulation, it was necessary to define the material properties, boundary conditions, and contact properties of the cartilages. For the material properties, a Young's modulus of 1.12 MPa and a Poisson's ratio of 0.49 were used for the cartilages.[37] For the boundary conditions, assuming no deformation at the surfaces between the bones and the cartilages due to highly rigid bones compared to cartilages,[38] the distal aspect of the metacarpal cartilage was constrained by kinematic coupling to a reference point on the F/E rotation axis, with the proximal aspect of the trapezium cartilage fixed (Figure 3). For the contact properties between the cartilages, a friction coefficient of 0.002 and a contact stiffness of 250 kPa/mm were used,[39,40] with penalty friction formulation and linear pressure–overclosure relationship applied to define the tangential and normal contact behaviors, respectively. Note that a finite sliding formulation with a surface-to-surface discretization method was used to define contact interaction for FE analysis. Moreover, for the FE simulation, the free mesh algorithm in ABAQUS software was used to mesh the cartilages with 3D 10-node tetrahedral elements (C3D10H), resulting in an average of 37,884 elements and 60,148 nodes for each cartilage. The quality of this mesh was evaluated by aspect ratio, which was 1.83 ± 0.05 and considered acceptable as it was below 5.

The optimal TMCJ posture was determined by analyzing joint contact pressure in various TMCJ postures using the FEM with ABAQUS software. To enable users to perform daily activities after immobilizing the TMCJ, the optimal TMCJ posture was identified among postures that were abducted and flexed relative to the "neutral" posture. Therefore, the metacarpal cartilage in the FE TMCJ model was abducted and flexed via the determined A/A and F/E rotation axes under a static condition. Specifically,

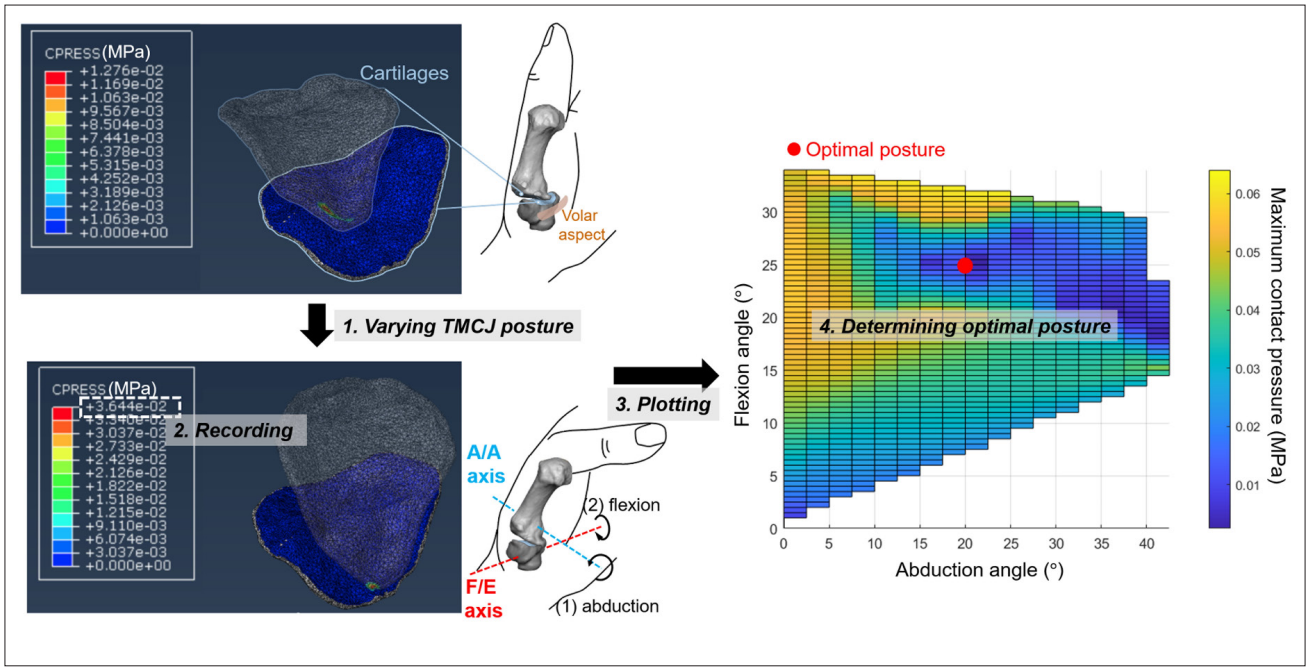


**Figure 3.** The FEM is applied to the constructed FE TMCJ model to determine the optimal posture that minimizes biomechanical joint contact pressure on the cartilage. Abbreviations: A/A, abduction-adduction; F/E, Flexion-extension; FE, finite element; FEM, finite element method; TMCJ: Trapeziometacarpal joint.

the metacarpal cartilage was first rotated around the A/A rotation axis for abduction before the FE simulation, and the abducted cartilage was then set to rotate around the F/E rotation axis by adjusting the kinematics of its coupled reference point for the simulation, while estimating joint contact pressure between the cartilages. The FEM-based maximum joint contact pressure was recorded for each TMCJ posture generated by the rotations. Subsequently, the optimal posture, which exhibited minimal joint contact pressure among various postures, was determined (Figure 3).

### 2.4. Fabrication of the orthosis via 3D printing

The orthosis was designed based on a 3D hand model posed in the optimal posture to immobilize the TMCJ in that posture during splinting. A 3D hand model posing the optimal posture was built prior to modeling the orthosis. Specifically, the overall hand geometry was reconstructed from CT images of the "neutral" posture. The thumb skin was then separated and rotated around the determined rotation axes to achieve the optimal posture. The orthosis was modeled to cover the built 3D hand model using Geomagic Freeform software (Figure 1). The modeled orthosis was then rigidly fabricated using a 3D printer (Cubicon Single; Hyvision System, Inc., South Korea) with a plastic material (ABS; Hyvision System, Inc., South Korea) and covered with fabric and straps.

### 2.5. Experimental evaluation

Orthoses fabricated using 3D printing were evaluated for their capability to maintain a targeted TMCJ posture and provide satisfactory wearing comfort during splinting (Figure 4). Two healthy subjects (healthy group [H1–2]; demographics listed in Table 1) were recruited for the evaluation. They were guided to fix the TMCJ in one of the flexion-abduction postures while maintaining the other fingers in a fully extended posture during 3D scanning using a 3D scanner (Sense2; 3D Systems Inc., USA). Subsequently, the orthosis was designed to cover the 3D hand model reconstructed from the 3D scanning data to maintain the scanned flexion-abduction posture as the targeted posture during splinting. After donning the 3D-printed orthosis, the TMCJ angles (i.e., $\theta_{sag}$ and $\theta_{cor}$) were measured in the sagittal and coronal planes of the hand and compared to the angles measured from the printed 3D hand model. Note that the TMCJ angles were measured using a reflective marker-based motion capture system (Figure 4). Additionally, the subjects were asked to evaluate their satisfaction with wearing comfort by marking a 10-cm-long line.

Six patients (experimental [S1–4] and control [C1–2] groups; demographics listed in Table 1), diagnosed with TMCJ OA and consented to participate in this study, were recruited to evaluate the orthosis. Exclusion criteria were patients with inflammatory arthritis or neuromuscular

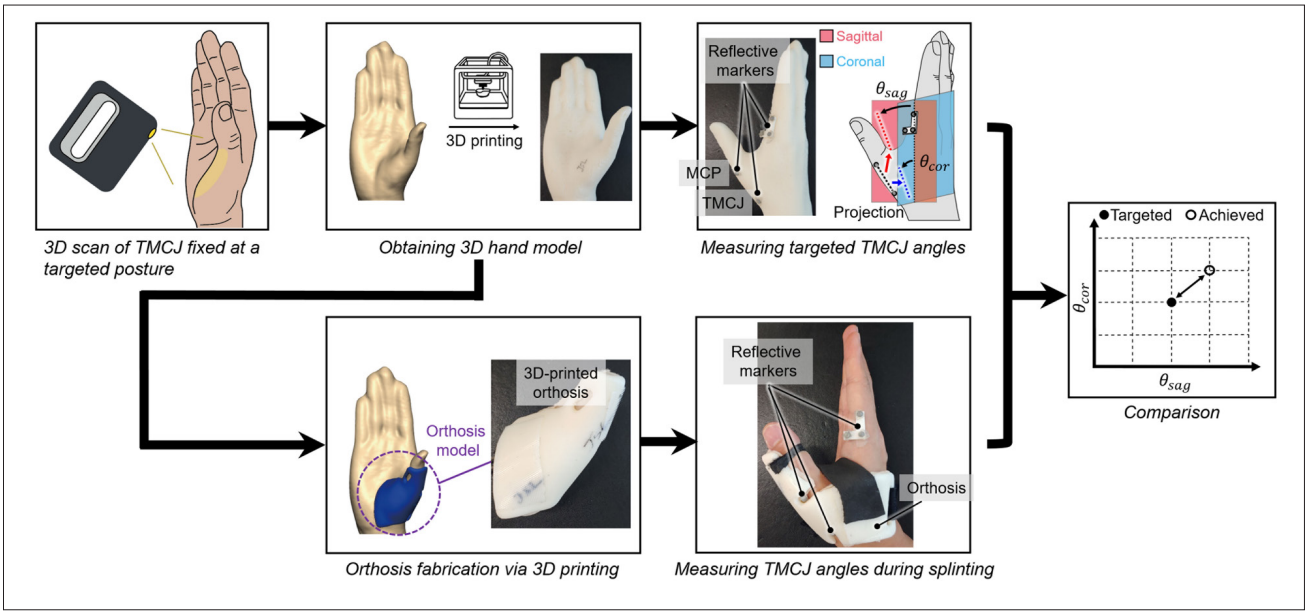


**Figure 4.** The experiment procedure used to evaluate the capability of the orthosis in maintaining the targeted TMCJ posture during splinting. Abbreviations: MCP, Metacarpophalangeal joint; TMCJ: trapeziometacarpal joint.

**Table 1. Demographics of the enrolled subjects.**

| Participant number | Sex | Age (years) | Duration of pain (years) | Hand dominance | Involved hand | Eaton classification |
|---|---|---|---|---|---|---|
| H1 | Male | 26 | - | Right | - | - |
| H2 | Female | 30 | - | Right | - | - |
| S1 | Female | 51 | 1.2 | Right | Right | 3 |
| S2 | Female | 78 | 1.5 | Right | Left | 3 |
| S3 | Female | 51 | 0.8 | Left | Left | 3 |
| S4 | Female | 58 | 5.0 | Right | Left | 3 |
| C1 | Female | 53 | 1.0 | Right | Left | 2 |
| C2 | Female | 73 | 2.1 | Right | Left | 4 |

disease. The orthosis for S1–4 was designed to fix the TMCJ to the optimal posture. All subjects were instructed to wear the orthosis as much as possible for 8 weeks. For comparison, C1–2 was provided with an orthosis that fixed the TMCJ in a non-optimal but comfortable posture, as conventional orthopedic treatment. Determining the most comfortable TMCJ posture was challenging due to the difficulty of distinguishing comfort levels among multiple comfortable postures based on subjective feelings. Therefore, splinting was performed using one of the postures that patients reported as comfortable and adopted in previous studies.[12] The research was approved by the Institutional Review Board of Seoul National University Bundang Hospital (No. B-2012-654-301), and written consent was obtained from each subject after the experiment was explained. The following criteria were measured for the evaluation:

(i) Disabilities of the arm, shoulder, and hand (DASH) and visual analog scale (VAS) scores: Before the application of the orthosis, all patients completed a DASH questionnaire. This self-administered questionnaire consists of 30 items and objectively measures the functional status and symptoms of patients with musculoskeletal disorders of the upper limb. The possible DASH score ranges from 0 (asymptomatic) to 100 (totally incapacitated).[41] At the follow-up visit 8 weeks after the application, the DASH questionnaire was re-administered. Conversely, VAS ranging from 0 to 10 was used to evaluate pain relief by the orthosis. Pain at rest ($VAS_{rest}$) and maximal pain ($VAS_{max}$) occurring

during daily activities that patients typically feel were measured at the initial and follow-up visits. Note that an decrease in the VAS score of 1 or more indicates an improvement in pain status.[42]

(ii) Pinch strength: Before the application of the orthosis, all patients were evaluated for their pinch strength using a pinch gauge (Asimow Engineering, USA). With their shoulder, elbow, forearm, and wrist in a neutral position, three consecutive attempts were made to measure pinch strength (kg), with a 1 min interval between each attempt.[43] The maximum value obtained was recorded. At the follow-up visit, the pinch strength was re-examined in the same manner.

(iii) Wearing comfort: The patients were asked to mark a 10-cm-long line to indicate their satisfaction with the orthosis in terms the wearing comfort.

## 3. Results

It was demonstrated by healthy subjects that orthoses fabricated via 3D printing can maintain the targeted TMCJ posture while providing satisfactory wearing comfort during splinting. The measured TMCJ angles during splinting and the targeted TMCJ angles are summarized in Figure 5. The TMCJ posture maintained by the orthosis was comparable to that of the 3D-scanned hand. The difference between the targeted and achieved TMCJ angles was 3.8° ± 0.4°. Moreover, the subjects scored 8.0 ± 1.4 for the wearing comfort of the 3D-printed orthosis.

The joint contact pressure analysis results and optimal TMCJ postures of patients are presented in Figure 6. Joint contact pressure was minimized at the optimal posture, while it increased as the postures deviated from the optimal posture. The joint contact pressure was considered valid, as the FEM-based pressure at a lateral pinch posture was comparable to the reported pressure measured in the lateral pinch posture at rest, which ranged from 6.0E-3 to 1.1E-2 MPa.[44] Additionally, the contact pattern during cartilage gliding matched the previous results.[45,46] Specifically, joint contact pressure areas move toward the volar aspect of cartilages as the flexion angle increases.

The optimal and immobilized postures were designed to coincide for S1–4, and these postures exhibited differences between individuals (Figure 6A). The flexion angle of the optimal posture was larger for S3 than for S1, S2, and S4, and the abduction angle varied between patients.

Differences were exhibited between the optimal and immobilized postures in the control group (Figure 6B). Joint contact pressures at the immobilized postures for C1 and C2 were similar, specifically 2.5E-2 and 3.9E-2 MPa, respectively. These pressures are only about half of the applied joint contact pressure (i.e., 7.8E-2 MPa) during lateral pinching with a grip force of 4.2 kg.[47]

Evaluation results of the orthoses are presented in Table 2. The orthosis for C1 was not assessed because C1 discontinued the orthotic treatment due to unrelieved pain at rest during splinting. Note that the Easton classification grade does not correlate with the $VAS_{rest}$ score measured before splinting, as confirmed in previous research.[21,48]

### 3.1. DASH and VAS scores

The $VAS_{rest}$ score improved for all S1–4, with a reduction of 1.8 ± 1.7. S1 and S2 reported no pain during splinting. The most significant decrease in the $VAS_{rest}$ score was observed for S4, who exhibited minimal joint contact pressure among patients. Moreover, despite the immobilization of the TMCJ, the DASH score decreased by 13.1 ± 5.4 for S2–4, indicating

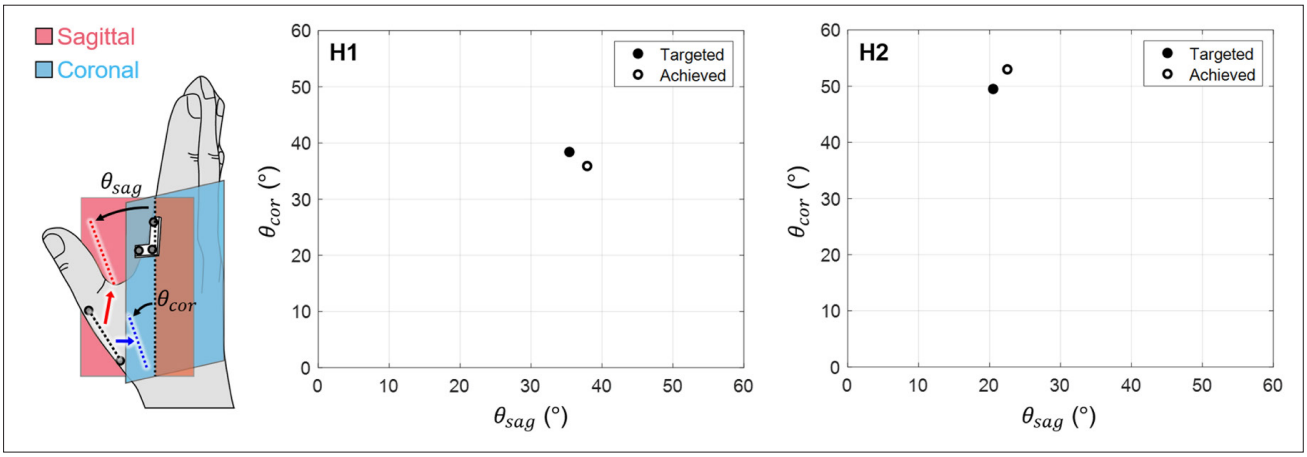


**Figure 5.** Measurement results of TMCJ angles for healthy subjects (H1 and H2) after donning the 3D-printed orthosis. The maintained TMCJ angles by the orthosis were comparable to the targeted TMCJ angles. Abbreviation: TMCJ, trapeziometacarpal joint.

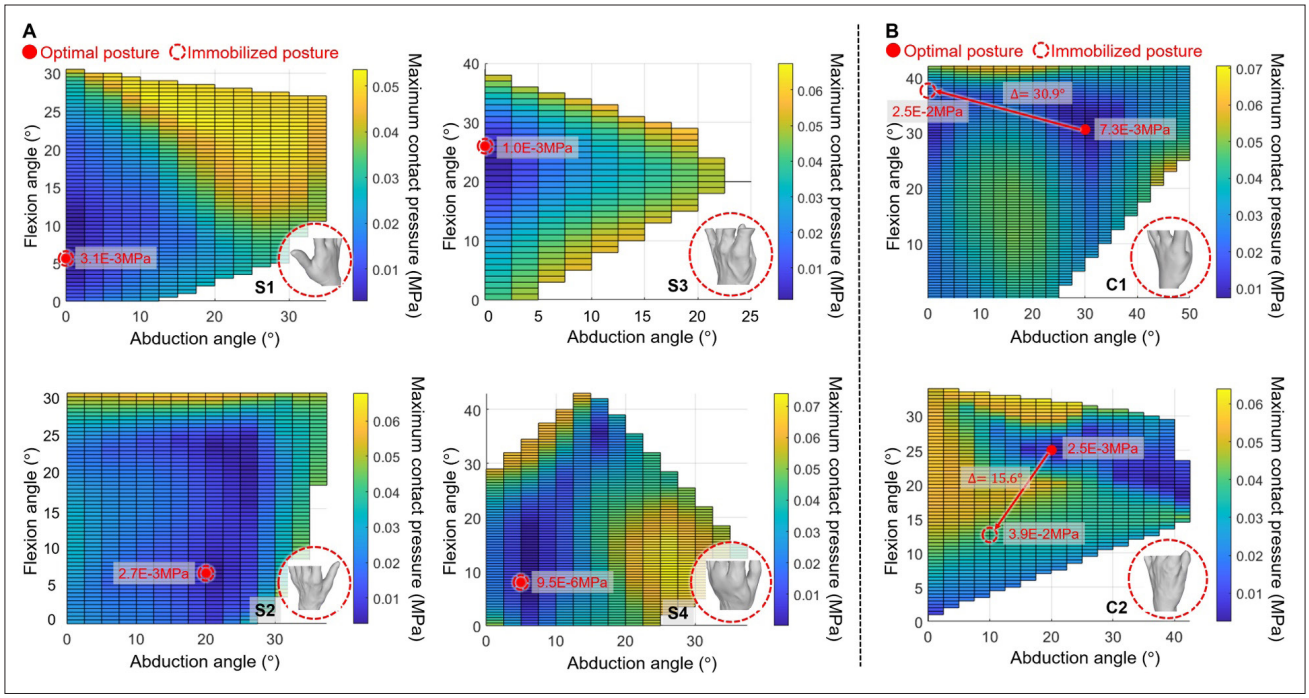


**Figure 6.** Analysis results of joint contact pressure for all patients. (A) The optimal and immobilized postures of the patients' orthosis in the experimental group. (B) The optimal and immobilized postures of the patients' orthosis in the control group.

**Table 2. Evaluation results of the patients' orthosis.**

| Participant number | Before splinting | | | | During splinting | | | | |
|---|---|---|---|---|---|---|---|---|---|
| | $VAS_{rest}$ | $VAS_{max}$ | DASH | Pinch (kg) | $VAS_{rest}$ | $VAS_{max}$ | DASH | Pinch (kg) | Wearing comfort |
| S1 | 0 | 7 | 22.5 | 4.8 | 0 | 4 | 63.6 | 8.8 | 8 |
| S2 | 1 | 4 | 50.0 | 5.3 | 0 | 3 | 43.1 | 5 | 8 |
| S3 | 3 | 4 | 31.8 | 4.8 | 1 | 4 | 15.9 | 4.5 | 9 |
| S4 | 6 | 8 | 41.5 | 5.4 | 2 | 5 | 25.0 | 5.4 | 10 |
| C1 | 4 | 7 | 36.4 | 5.8 | - | - | - | - | - |
| C2 | 1 | 4 | 15.9 | 5.3 | 0 | 4 | 11.4 | 5.1 | 9 |

Abbreviations: DASH, disabilities of arm, shoulder, and hand scores; VAS, visual analog scale.

an improvement in functional status possibly attributed to pain relief. Note that a TMCJ posture close to "neutral" would not be desirable for splinting due to the reported increase in the DASH score for S1, caused by difficulties in performing grasping with that posture. The $VAS_{max}$ score for S1–2 and S4 also decreased during splinting.

For C2, VAS and DASH scores displayed improvement. The $VAS_{rest}$ score decreased during splinting, while the $VAS_{max}$ score did not change. The DASH score also improved, decreasing from 15.9 to 11.4.

### 3.2. Pinch strength

Pinch strength displayed no significant change; it decreased by a small amount, 0.2 ± 0.1 kg, for S2–4 and C2. Muscle weakness during splinting, possibly due to infrequent use, might have led to a decrease in pinch strength, even though pain was relieved.[49,50] However, there was an increase in pinch strength for S1, from 4.8 to 8.8 kg. As S1 was hindered in performing daily activities by the orthosis, the thumb flexors might have been frequently used to exert force against the orthosis to release from the immobilized posture, thus preventing muscle weakness. Therefore, S1 might have been capable of performing grasping more powerfully after experiencing pain relief.

### 3.3. Wearing comfort

All patients reported satisfaction with the wearing comfort of the orthosis during splinting. The orthosis was rated 8.8 ± 1.0 by S1–4 and 9 by C2.

## 4. Discussion

This study proposes a novel 3D printing design process for a TMCJ orthosis, based on joint contact pressure obtained using a CT image-based FE TMCJ model. The primary objective of the orthosis is to ensure successful pain relief at rest during splinting by enabling patients to maintain the subject-specific optimal TMCJ posture that minimizes biomechanical joint contact pressure. Before designing the orthosis, the optimal TMCJ posture was individually determined through joint contact pressure analysis using a FE TMCJ model. The orthosis was then designed to cover a 3D hand model posed in the optimal TMCJ posture, enabling the orthosis to maintain the optimal posture during splinting. The orthosis was preliminarily applied to patients with moderate to severe TMCJ OA, and they all achieved pain relief at rest.

Immobilizing the TMCJ at comfortable postures determined during a brief hospital visit cannot ensure the achievement of pain relief during long-term splinting. Immobilization can typically relieve biomechanical cartilage wear due to restricted joint mobilization. Therefore, immobilization has been utilized for OA treatment through static orthoses.[9–11,13–15,17,18] However, high joint contact pressure in immobilized postures may lead to localized wear at cartilage contact areas due to slight allowed movement,[51] resulting in inflammatory response and pain.[52] Postures with this high joint contact pressure can be misperceived as comfortable, as confirmed in the control group. This could be attributed to the improved pain tolerance typically observed in patients within a hospital environment by reduced anxiety due to the presence of professional clinicians.[22,23] Thus, the comfortable posture determined solely by patients may not guarantee the long-term comfort of the orthosis. As a result of the high joint contact pressure, pain relief at rest failed for one of two patients in the control group, while another patient reported pain relief despite their similar high joint contact pressure values. Patients with high $VAS_{rest}$ scores of 3 or higher are reported to be vulnerable to experiencing increased pain during splinting,[48] and this vulnerability may result in the failure of pain relief for the patient with a high $VAS_{rest}$ score. Therefore, it would be desirable to minimize joint contact pressure in the immobilized posture to achieve pain relief at rest for patients, regardless of their $VAS_{rest}$ scores.

Immobilizing the TMCJ at the optimal posture may be beneficial in preventing the failure of pain relief. Reducing joint contact pressure is essential to minimize biomechanical wear on cartilages,[3,4] and this has been achieved in knee and hip joints by adjusting postures with the aid of FE joint models.[5–8] On the other hand, the TMCJ has been maintained in comfortable postures by orthoses without considering joint contact pressure, assuming that joint contact pressure is relieved with comfort.[9–11,13–15,17,18] However, TMCJ postures with high joint contact pressure can be misperceived as comfortable, as observed in patients in the control group. This may result in a high failure rate of pain relief, which ranges from 30% to 47%.[19–21] It would be desirable to avoid high joint contact pressure at the TMCJ by utilizing a CT-based individual FE model for TMCJ orthosis design. Thus, in this study, a CT image-based FE TMCJ model was applied to the orthosis design for minimum contact pressure. As a result, all four patients maintaining the optimal posture successfully achieved pain relief at rest during splinting, implying a reduction of joint contact pressure. Note that even patients with $VAS_{rest}$ scores of 3 or higher before splinting achieved pain relief at rest through the optimal posture. Despite the limited room for improvement in the recruited patients of our study due to their relatively low pain scores in the baseline assessment compared to those in other studies,[9–11,13–15] the improvement in pain was comparable to that of conventional orthoses[9–11,13–15] that had displayed a positive effect on pain relief. Note that the VAS score at rest during splinting was only $0.75 \pm 0.96$ in this study. Thus, it was believed that there is potential for enhancing pain relief performance, as evidenced by the successful pain relief achieved by all four patients, in contrast to the high failure rate observed with conventional orthoses. Due to this pain relief, functional status in daily activities demonstrated improvement, with no significant change in grip strength possibly due to muscle weakness, which aligns with the results of previous studies on conventional orthoses.[9–11,15]

The distant location of the applied joint contact pressure from cartilage lesions may be beneficial in relieving maximal pain measured as $VAS_{max}$ scores. Pain occurs when high pressure is applied to cartilage lesions, and the distribution of these cartilage lesions is reported to be varied for each patient.[53] In this study, cartilage lesions were expected to be located at the volar aspect for all patients, determined through the evaluation of subchondral sclerosis and bone spurs using CT images.[54] Moreover, it was anticipated that there would be more severe damage at cartilage areas closer to their volar edge.[2] Considering that joint contact pressure areas move towards the volar edge of cartilages as a flexion angle increases,[45,46] the optimal posture with a large flexion angle may result in high joint contact pressure applied to severely damaged cartilage areas during grasping, limiting the capability to relieve maximal pain for one patient in the experimental group. Both pain at rest and maximal pain may be alleviated with orthoses designed to apply minimal joint contact pressure to cartilage areas located far from lesions.

The compliance of TMCJ orthoses is important for users due to their long-term use. While soft materials can be used in the orthosis[17,18] to address the wearing discomfort experienced when using orthoses made from rigid materials, immobilizing the TMCJ posture may become challenging. Although the material used in the proposed orthosis was rigid, patients reported satisfaction with the wearing comfort after donning. The compliance of the orthosis was considered to be attributed to its design, which was based on individual hand geometry.[27,28] Additionally, thermoplastic pads commonly used in conventional orthoses can be utilized to fabricate the orthosis to maintain the optimal posture. The 3D hand model, posed in the optimal posture, can be 3D-printed and then covered with thermoplastic pads and fabric. These thermoplastic pads, covered with fabric, can also be employed to maintain the optimal posture during splinting.

The proposed orthosis design can be applied to static braces developed for the wrist OA. While the FEM has been utilized to analyze joint contact pressure at the wrist,[55,56] where OA commonly occurs, there are still limited studies on developing wrist OA braces designed based on a CT-based FE joint model for optimal postures.[57,58] The proposed orthosis design may aid in developing wrist OA braces for the optimal posture to achieve pain relief.

This study has limitations. The proposed orthosis was evaluated with a limited number of patients, and the evaluation was conducted only after 8 weeks of splinting. Nevertheless, we believe that the orthosis can reduce the failure rate of pain relief for patients with TMCJ OA, whether used for a shorter or longer period of splinting, due to its design, which reduces biomechanical joint contact pressure. Moreover, the locations of the rotation axes were fixed in the FE model, which may not be applicable to patients exhibiting significant translation of the metacarpal during movement due to severe structural instability.

## 5. Conclusion

This study presents a novel patient-specific design for a TMCJ orthosis aimed at achieving successful pain relief during splinting by using 3D printing technology. Despite the possibility of estimating joint contact pressure at the TMCJ using FE joint models, conventional TMCJ orthoses have been designed solely based on subjective comfort reported by patients without considering the contact pressure. To ensure pain relief during splinting, we introduce a TMCJ orthosis design using CT image-based FE TMCJ models to immobilize the TMCJ in the optimal posture that minimizes biomechanical joint contact pressure. The proposed 3D-printed TMCJ orthosis was applied to patients with OA and preliminarily demonstrated its capability in relieving pain for all patients, implying a reduction of joint contact pressure at the optimal posture.

By using 3D bioprinting technology and a subject-specific FE model, immobilization of the TMCJ in a subject-specific optimal posture that minimizes joint contact pressure is achieved for successful pain relief during splinting; otherwise, pain relief may fail due to high pressure. An orthosis designed solely based on subjective reports on comfort could not guarantee pain relief (i.e., one subject in the control group quit the study due to severe pain), which may be attributed to the high contact pressure. To reduce the failure rate of pain relief in clinical treatment, it would be desirable for the orthosis to be designed with the aid of a CT image-based FE model to maintain the TMCJ in the optimal posture. This optimal posture was found to vary between individuals, necessitating the patient-specific TMCJ orthosis design, which could be facilitated by 3D printing technology.

In future studies, the proposed orthosis will be evaluated on a sufficient number of patients over various splinting periods to demonstrate its capability to improve pain relief with strong statistical power compared to conventional TMCJ orthoses. Moreover, the material of the orthosis, which is ABS covered by fabrics in this study, will be improved for comfort after skin pressure distribution analysis with various 3D-printable materials, such as flexible thermoplastic polyurethane (TPU), further simplifying the fabrication process. Its capability to relieve pain even after doffing the orthosis worn for a longer period will be also assessed.

## Acknowledgments

None.

## Funding

This work was supported in part by the Korea Research Institute for defense Technology planning and advancedment(KRIT) grant funded by the Korea government (DAPA(Defense Acquisition Program Administration)) (No. 21-107-E00-009-02, “Realtime complex battlefield situation awareness technology”) and in part by the funding from the Korea government Ministry of Science and ICT (grant number RS-2023-00209251).

## Conflict of interest

The authors declare they have no competing interests.

## Author contributions

*Conceptualization:* All authors
*Formal analysis:* Chan Beom Park, Ji Sup Hwang
*Investigation:* Chan Beom Park, Ji Sup Hwang
*Methodology:* Chan Beom Park, Ji Sup Hwang
*Supervision:* Hyun Sik Gong, Hyung-Soon Park
*Writing – original draft:* Chan Beom Park, Ji Sup Hwang
*Writing – review & editing:* Hyun Sik Gong, Hyung-Soon Park

## Ethics approval and consent to participate

The research was approved by the Institutional Review Board of Seoul National University Bundang Hospital (No. B-2012-654-301), and written consent was obtained from each subject after the experiment was explained.

## Consent for publication

Written consent for publication was obtained.

## Availability of data

The data that support the findings of this study are available from the corresponding authors upon reasonable request.

## References


1. Gillis J, Calder K, Williams J. Review of thumb carpometacarpal arthritis classification, treatment and outcomes. *Can J Plast Surg.* 2011;19(4):134-138. doi: 10.1177/229255031101900409
2. Koff MF, Ugwonali OF, Strauch RJ, Rosenwasser MP, Ateshian GA, Mow VC. Sequential wear patterns of the articular cartilage of the thumb carpometacarpal joint in osteoarthritis. *J Hand Surg Am.* 2003;28(4):597-604. doi: 10.1016/S0363-5023(03)00145-X
3. Fontana L, Neel S, Claise J-M, Ughetto S, Catilina P. Osteoarthritis of the thumb carpometacarpal joint in women and occupational risk factors: a case–control study. *J Hand Surg Am*. 2007;32(4):459-465. doi: 10.1016/j.jhsa.2007.01.014
4. Fergusson CM. The aetiology of osteoarthritis. *Postgrad Med J.* 1987;63(740):439. doi: 10.1136/pgmj.63.740.439
5. Spierings J, Van Den Hengel M, Janssen RP, Van Rietbergen B, Ito K, Foolen J. Knee instability caused by altered graft mechanical properties after anterior cruciate ligament reconstruction: the early onset of osteoarthritis? *Front Bioeng Biotechnol*. 2023;11:1244954. doi: 10.3389/fbioe.2023.1244954
6. Wang Y, Fan Y, Zhang M. Comparison of stress on knee cartilage during kneeling and standing using finite element models. *Med Eng Phys.* 2014;36(4):439-447. doi: 10.1016/j.medengphy.2014.01.004
7. Esrafilian A, Stenroth L, Mononen M, Tanska P, Avela J, Korhonen R. EMG-assisted muscle force driven finite element model of the knee joint with fibril-reinforced poroelastic cartilages and menisci. *Sci Rep*. 2020;10(1):3026. doi: 10.1038/s41598-020-59602-2
8. Zhang Z, Sui D, Qin H, Li H, Zhang Z. Contact pressure distribution of the hip joint during closed reduction of developmental dysplasia of the hip: a patient-specific finite element analysis. *BMC Musculoskelet Disord.* 2020;21(600):1-12. doi: 10.1186/s12891-020-03602-w
9. Wajon A, Ada L. No difference between two splint and exercise regimens for people with osteoarthritis of the thumb: a randomised controlled trial. *Aust J Physiother.* 2005;51(4):245-249. doi: 10.1016/S0004-9514(05)70005-2
10. Carreira ACG, Jones A, Natour J. Assessment of the effectiveness of a functional splint for osteoarthritis of the trapeziometacarpal joint on the dominant hand: a randomized controlled study. *J Rehabil Med*. 2010; 42(5):469-474. doi: 10.2340/16501977-0542
11. Weiss S, Lastayo P, Mills A, Bramlet D. Prospective analysis of splinting the first carpometacarpal joint: an objective, subjective, and radiographic assessment. *J Hand Surg.* 2000;13(3):218-227. doi: 10.1016/S0894-1130(00)80005-8
12. Colditz JC. The biomechanics of a thumb carpometacarpal immobilization splint: design and fitting. *J Hand Ther.* 2000;13(3):228-235. doi: 10.1016/S0894-1130(00)80006-X
13. Cantero-Téllez R, Villafañe JH, Valdes K, Berjano P. Effect of immobilization of metacarpophalangeal joint in thumb carpometacarpal osteoarthritis on pain and function. A quasi-experimental trial. *J Hand Ther*. 2018;31(1):68-73. doi: 10.1016/j.jht.2016.11.005
14. Bani MA, Arazpour M, Kashani RV, Mousavi ME, Maleki M, Hutchins SW. The effect of custom-made splints in patients with the first carpometacarpal joint osteoarthritis. *Prosthet Orthot Int*. 2013;37(2):139-144. doi: 10.1177/0309364612454047
15. Eyiis E, Mathijssen NM, Kok P, Sluijter J, Kraan GA. Three-dimensional printed customized versus conventional plaster brace for trapeziometacarpal osteoarthritis: a randomized controlled crossover trial. *J Hand Surg Eur Vol* 2023;48(5):412-418. doi: 10.1177/17531934221146864
16. Chu C-H, Wang I-J, Sun J-R, Liu C-H. Customized designs of short thumb orthoses using 3D hand parametric models. *Assist Technol*. 2022;34(1):104-111. doi: 10.1080/10400435.2019.1709917

17. Hermann M, Nilsen T, Eriksen CS, Slatkowsky-Christensen B, Haugen IK, Kjeken I. Effects of a soft prefabricated thumb orthosis in carpometacarpal osteoarthritis. *Scand J Occup Ther*. 2014;21(1):31-39.
doi: 10.3109/11038128.2013.851735

18. Becker SJE, Bot AGJ, Curley SE, Jupiter JB, Ring D. A prospective randomized comparison of neoprene vs thermoplast hand-based thumb spica splinting for trapeziometacarpal arthrosis. *Osteoarthr Cartil Open*. 2013;21(5):668-675.
doi: 10.1016/j.joca.2013.02.006

19. Tsehaie J, Spekreijse KR, Wouters RM, et al. Predicting outcome after hand orthosis and hand therapy for thumb carpometacarpal osteoarthritis: a prospective study. *Arch Phys Med Rehabil*. 2019;100(5):844-850.
doi: 10.1016/j.apmr.2018.08.192

20. Berggren M, Joost-Davidsson A, Lindstrand J, Nylander G, Povlsen B. Reduction in the need for operation after conservative treatment of osteoarthritis of the first carpometacarpal joint: a seven year prospective study. *Scand J Plast Reconstr Surg Hand Surg*. 2001;35(4):415-417.
doi: 10.1080/028443101317149381

21. Suresh V, Frost CM, Lifchez SD. Selective thumb carpometacarpal joint denervation for painful arthritis: follow-up of long-term clinical outcomes. *J Hand Surg Glob Online*. 2023;5(1):108-111.
doi: 10.1016/j.jhsg.2022.02.005

22. Karacabay K, Savci A, Hergul FK. Investigating relationships between pain, comfort, anxiety and depression in surgical patients. *Cyprus J Med Sci*. 2022;7:40-47.
doi: 10.4274/cjms.2020.1758

23. Schloemann D, Hammert WC, Liu S, Bernstein DN, Calfee RP. Risk factors for failed nonsurgical treatment resulting in surgery on thumb carpometacarpal arthritis. *J Hand Surg*. 2021;46(6):471-477.
doi: 10.1016/j.jhsa.2021.02.009

24. Xiao YP, Xu HJ, Liao W, Li ZH. Clinical application of instant 3D printed cast versus polymer orthosis in the treatment of colles fracture: a randomized controlled trial. *BMC Musculoskelet Disord*. 2024;25(1):104.
doi: 10.1186/s12891-024-07212-8

25. Cho JE, Seo KJ, Ha S, Kim H. Effects of community ambulation training with 3D-printed ankle–foot orthosis on gait and functional improvements: a case series of three stroke survivors. *Front Neurol*. 2023;14:1138807.
doi: 10.3389/fneur.2023.1138807

26. Peng C, Tran P, Lalor S, Tirosh O, Rutz E. Tuning the mechanical responses of 3D-printed ankle-foot orthoses: a numerical study. *Int J Bioprint*. 2024; 10(3):3390.
doi: 10.36922/ijb.3390

27. Park CB, Park H-S. Portable 3D-printed hand orthosis with spatial stiffness distribution personalized for assisting grasping in daily living. *Front Bioeng Biotechnol*. 2023;11:895745.
doi: 10.3389/fbioe.2023.895745

28. Park CB, Hwang JS, Gong HS, Park H-S. A lightweight dynamic hand orthosis with sequential joint flexion movement for postoperative rehabilitation of flexor tendon repair surgery. *IEEE Trans Neural Syst Rehabil Eng*. 2024;32:994-1004.
doi: 10.1109/TNSRE.2024.3367990

29. Hollister A, Buford WL, Myers LM, Giurintano DJ, Novick A. The axes of rotation of the thumb carpometacarpal joint. *J Orthop Res*. 1992;10(3):454-460.
doi: 10.1002/jor.1100100319

30. D'Agostino P, Dourthe B, Kerkhof F, Stockmans F, Vereecke EE. In vivo kinematics of the thumb during flexion and adduction motion: evidence for a screw-home mechanism. *J. Orthop. Res*. 2017;35(7):1556-1564.
doi: 10.1002/jor.23421

31. Santos VJ, Valero-Cuevas FJ. Reported anatomical variability naturally leads to multimodal distributions of Denavit-Hartenberg parameters for the human thumb. *IEEE Trans Biomed Eng*. 2006;53(2):155-163.
doi: 10.1109/TBME.2005.862537

32. O'Brien VH, Giveans MR. Effects of a dynamic stability approach in conservative intervention of the carpometacarpal joint of the thumb: a retrospective study. *J Hand Ther*. 2013;26(1):44-52.
doi: 10.1016/j.jht.2012.10.005

33. Akiyama K, Sakai T, Koyanagi J, Murase T, Yoshikawa H, Sugamoto K. Three-dimensional distribution of articular cartilage thickness in the elderly cadaveric acetabulum: a new method using three-dimensional digitizer and CT. *Osteoarthr Cartil Open*. 2010;18(6):795-802.
doi: 10.1016/j.joca.2010.03.007

34. Prionas ND, Ray S, Boone JM. Volume assessment accuracy in computed tomography: a phantom study. *J Appl Clin Med Phys*. 2010;11(2):168-180.
doi: 10.1120/jacmp.v11i2.3037

35. Miura T, Ohe T, Masuko T. Comparative in vivo kinematic analysis of normal and osteoarthritic trapeziometacarpal joints. *J Hand Surg*. 2004;29(2):252-257.
doi: 10.1016/j.jhsa.2003.11.002

36. Hamann N, Heidemann J, Heinrich K, et al. Effect of carpometacarpal joint osteoarthritis, sex, and handedness on thumb in vivo kinematics. *J Hand Surg*. 2014; 39(11):2161-2167.
doi: 10.1016/j.jhsa.2014.08.012

37. Butz KD, Merrell G, Nauman EA. A three-dimensional finite element analysis of finger joint stresses in the MCP joint while performing common tasks. *Hand*. 2012;7(3): 341-345.
doi: 10.1007/s11552-012-9430-4

38. Peters AE, Akhatar R, Comerford EJ, Bates KT. The effect of ageing and osteoarthritis on the mechanical properties of cartilage and bone in the human knee joint. *Sci Rep.* 2018;8(1):5931.
doi: 10.1038/s41598-018-24258-6

39. Guilak F. The slippery slope of arthritis. *Arthritis Rheumatol.* 2005;52(6):1632-1633.
doi: 10.1002/art.21051

40. Yuh C, Laurent MP, Espinosa-Marzal RM, Chubinskaya S, Wimmer MA. Transient stiffening of cartilage during joint articulation: a microindentation study. *J Mech Behav Biomed Mater.* 2021;113:104113.
doi: 10.1016/j.jmbbm.2020.104113

41. Lee J-Y, Lim J-Y, Oh JH, Ko Y-M. Cross-cultural adaptation and clinical evaluation of a Korean version of the disabilities of arm, shoulder, and hand outcome questionnaire (K-DASH). *J Shoulder Elbow Surg.* 2008;17(4):570-574.
doi: 10.1016/j.jse.2007.12.005

42. Myles P, Myles D, Galagher W, et al. Measuring acute postoperative pain using the visual analog scale: the minimal clinically important difference and patient acceptable symptom state. *Br J Anaesth.* 2017;118(3):424-429.
doi: 10.1093/bja/aew466

43. Günther C, Bürger A, Rickert M, Schulz, C. Key pinch in healthy adults: normative values. *J Hand Surg Eur Vol.* 2008;33(2):144-148.
doi: 10.1177/1753193408087031

44. Cheema T, Salas C, Morrell N, Lansing L, Taha MMR, Mercer D. Opening wedge trapezial osteotomy as possible treatment for early trapeziometacarpal osteoarthritis: a biomechanical investigation of radial subluxation, contact area, and contact pressure. *J Hand Surg.* 2012; 37(4):699-705.
doi: 10.1016/j.jhsa.2012.01.013

45. Ateshian GA, Ark JW, Rosenwasser MP, Pawluk RJ, Soslowsky LJ, Mow VC. Contact areas in the thumb carpometacarpal joint. *J Orthop Res.* 1995; 13(3):450-458.
doi: 10.1002/jor.1100130320

46. Momose T, Nakatsuchi Y, Saitoh S. Contact area of the trapeziometacarpal joint. *J Hand Surg.* 1999;24(3): 491-495.
doi: 10.1053/jhsu.1999.0491

47. Hwang JS, Li Q, Kim J. A quantitative measurement of trapeziometacarpal joint pressure using a cadaveric model of lateral pinch. *J Orthop Res.* 2022;40(7):1523-1528.
doi: 10.1002/jor.25188

48. Nishimura K, Uehara K, Miura T, Ohe T, Tanaka S, Morizaki Y. Factors associated with surgical intervention for osteoarthritis of the thumb carpometacarpal joint. *J Hand Surg.* 2021;46(9):817-e1.
doi: 10.1016/j.jhsa.2021.01.009

49. Spaans AJ, Van Minnen LP, Kon M, Schuurman AH, Schreuders AT, Vermeulen GM. Conservative treatment of thumb base osteoarthritis: a systematic review. *J Hand Surg.* 2015;40(1):16-21.
doi: 10.1016/j.jhsa.2014.08.047

50. Suetta C, Hvid LG, Justesen L, et al. Effects of aging on human skeletal muscle after immobilization and retraining. *J Appl Physiol.* 2009;107(4):1172-1180.
doi: 10.1152/japplphysiol.00290.2009

51. Vanneste M, Stockmans F, Vereecke EE. The effect of orthoses on the kinematics of the trapeziometacarpal, scaphotrapeziotrapezoidal, and radioscaphoid joints. *J Orthop Res.* 2021;39(1):196-203.
doi: 10.1002/jor.24700

52. Estell EG, Silverstein AM, Stefani RM, et al. Cartilage wear particles induce an inflammatory response similar to cytokines in human fibroblast-Like Synoviocytes. *J Orthop Res.* 2019;37(9):1979-1987.
doi: 10.1002/jor.24340

53. Bae KJ, Jang HS, Gong HS, Kang Y, Kim J, Baek GH. Prevalence and distribution of MRI abnormalities in the articular cartilage and supporting ligaments in patients with early clinical stage first carpometacarpal joint osteoarthritis. *Skeletal Radiol.* 2020;49: 1089-1097.
doi: 10.1007/s00256-020-03383-2

54. Hwang JS, Lee HS, Gong HS. Three-dimensional analysis of the trapezium subchondral bone and its association with trapeziometacarpal joint osteoarthritis. *Calcif Tissue Int.* 2023;112(3):320-327.
doi: 10.1007/s00223-022-01040-5

55. Ledoux P, Lamblin D, Wuilbaut A, Schuind F. A finite-element analysis of Kienböck's disease. *J Hand Surg Eur Vol.* 2008;33(3):286-291.
doi: 10.1177/1753193408090757

56. Camus EJ, Aimar A, Van Overstraeten L, Schuind F, Innocenti B. Lunate loads following different osteotomies used to treat Kienböck's disease: a 3D finite element analysis. *Clin Biomech.* 2020;78:105090.
doi: 10.1016/j.clinbiomech.2020.105090

57. Van der Windt JW, Akkerman W, Hofstra M, Meussen P. Reduced pain and improved daily activities for individuals with hand osteoarthritis using a silicone wrist hand orthosis. *J Hand Ther.* 2023;36(3):669-677.
doi: 10.1016/j.jht.2022.09.003

58. Valdes K, Marik T. A systematic review of conservative interventions for osteoarthritis of the hand. *J Hand Ther.* 2010;23(4):334-351.
doi: 10.1016/j.jht.2010.05.001